

# ULRR

## Two-phase flow regime identification through local temperature mapping

Item Type	Article
Authors	O'Donovan, Alan;Grimes, Ronan
Citation	Experimental Thermal and Fluid Science;115, 110077
Publisher	Elsevier
Download date	2026-04-10 15:10:55
Item License	<a href="https://creativecommons.org/licenses/by-nc-sa/1.0/">https://creativecommons.org/licenses/by-nc-sa/1.0/</a>
Link to Item	<a href="https://hdl.handle.net/10344/8660">https://hdl.handle.net/10344/8660</a>

## Journal Pre-proofs

Two-phase flow regime identification through local temperature mapping

Alan O'Donovan, Ronan Grimes

PII: S0894-1777(19)31215-4

DOI: <https://doi.org/10.1016/j.expthermflusci.2020.110077>

Reference: ETF 110077

To appear in: *Experimental Thermal and Fluid Science*

Received Date: 29 July 2019

Revised Date: 31 December 2019

Accepted Date: 31 January 2020

Please cite this article as: A. O'Donovan, R. Grimes, Two-phase flow regime identification through local temperature mapping, *Experimental Thermal and Fluid Science* (2020), doi: <https://doi.org/10.1016/j.expthermflusci.2020.110077>

This is a PDF file of an article that has undergone enhancements after acceptance, such as the addition of a cover page and metadata, and formatting for readability, but it is not yet the definitive version of record. This version will undergo additional copyediting, typesetting and review before it is published in its final form, but we are providing this version to give early visibility of the article. Please note that, during the production process, errors may be discovered which could affect the content, and all legal disclaimers that apply to the journal pertain.

© 2020 Published by Elsevier Inc.



# Two-phase flow regime identification through local temperature mapping

Alan O'Donovan<sup>a,\*</sup>, Ronan Grimes<sup>b</sup>

<sup>a</sup>Department of Mechanical & Automobile Engineering, Limerick Institute of Technology, Limerick, Ireland.

<sup>b</sup>Bernal Institute, School of Engineering, University of Limerick, Limerick, Ireland.

## Abstract

Two-phase flows underpin some of our most ubiquitous technologies, ranging from micro-scale liquid-liquid cooling of electronics to macro-scale liquid-vapour boiling and condensation in thermal power plants. Establishing the morphology of a two-phase flow, under a prescribed set of conditions, is considered particularly important in the design stage. As the pressure loss and heat transfer characteristics of a two-phase flow are intimately linked to the fluidic arrangement, knowledge of the prevailing flow topology enhances understanding, and can lead to the development of flow-specific correlations and/or models. This paper presents a novel experimental measurement technique for identifying the predominant two-phase flow regime in a circular tube. Specifically, the investigation presented in this paper focuses on condensing flows of steam, at typical Rankine cycle cooling conditions. However, it is proposed that the experimental arrangement and methodology can be applied to any two-phase flow scenario. The approach presented herein employs a temperature measurement platform - composed from localised instrumentation - to measure the temperature drop, associated with the presence of a liquid phase, at any point in the tube. Through analysis and interpretation of local temperature difference measurements around the inside tube circumference, and along the tube length, the predominant flow regime can be identified. In this study, measurements were taken from a 25 mm internal diameter round tube, with steam flow rates in the range of 0.42 - 0.94 g·s<sup>-1</sup>. The flow regime was seen to transition from an annular-type profile nearest the tube inlet to a stratified-wavy topology towards the tube exit in all instances.

*Keywords:* condensation, two-phase flow, flow regime, flow mapping

## Nomenclature

$L$	tube length, m
$\dot{m}$	mass flow rate, kg·s <sup>-1</sup>
$P$	pressure, N·m <sup>-2</sup>
$\dot{Q}$	heat transfer rate, J·s <sup>-1</sup>
$Re$	Reynolds number, -
$r$	radial ordinate, m
$T$	temperature, K
$x$	steam quality, -
$z$	axial ordinate, m

## Greek Symbols

$\Delta T$	temperature difference, K
$\theta$	azimuthal ordinate, deg
$\sigma$	standard deviation, K

## Subscripts

$a$	air
$c$	condensate
$s$	steam
$sat$	saturation
$v$	vapour
$\infty$	ambient

## 1. Introduction

Two-phase flows are amongst the more complex transport mechanisms encountered in engineering applications. In addition to existing single-phase phenomena, including the transition to

\*Corresponding author

Email addresses: alan.odonovan@lit.ie (Alan O'Donovan), ronan.grimes@ul.ie (Ronan Grimes)

turbulence, three-dimensional behaviour, and unsteadiness, the presence of a second phase imparts complexities arising from the mass, momentum, and energy exchange which takes place between the phases. Interfacial effects, such as the motion and deformation of the interface, and the wetting characteristics of the liquid phase on the boundary surface, are unique features which distinguish two-phase flows from the more relatively straightforward single-phase cases. Despite this, and in some cases because of this, two-phase flows underpin some of our most ubiquitous technologies, ranging from the micro-scale liquid-liquid cooling of electronics to macro-scale liquid-vapour boiling and condensation in thermal power plants. As a result of such widespread and diverse application, two-phase flows have been the subject of considerable research efforts, with an emphasis on characterising the associated pressure drop and heat transfer mechanisms.

In two-phase flows, the pressure drop and heat transfer characteristics are intimately linked to the specific arrangement of the phases. Hence, it is generally recognised that a greater understanding of the flow regime behaviour can lead to the development of more accurate pressure drop and heat transfer predictive techniques. However, the vast majority of two-phase pressure drop correlations in the literature [1, 2, 3, 4] are purely empirical, without any reference to the flow regimes under consideration. Owing to this, there tends to be a large disparity in the prediction of pressure drop between the various correlations. More recent efforts in this field by Quibén and Thome [5] have shown that increased accuracy in pressure drop calculations can be achieved by consideration of the specific flow regime. It is expected that such studies, where calculation methods are based on flow regimes, will ultimately supersede those which do not account for the influence of flow regimes. The ability to identify flow regimes, and develop flow-specific correlations as a result, should lead to greater accuracy in the prediction of two-phase pressure drop and heat transfer coefficient.

In many cases, the flow regime of a given two-phase flow can be easily established from a flow pattern map, of which many different variants exist in the literature. These maps graphically describe the flow regimes by separating a two-dimensional space into a series of distinct regions, with each region corresponding to a particular flow regime. Some of the most popular flow maps in the literature are those of Baker [6], Hewitt and Roberts [7], Mandhane et al.

[8], and Taitel and Dukler [9]. Whilst commonly cited in two-phase studies, the applicability of these maps is, however, limited by their underlying database. Most flow pattern maps have been developed for adiabatic conditions, and extrapolation of such maps to diabatic conditions is unreliable and is not recommended. More recently, specific diabatic flow pattern maps have been developed by Kattan et al. [10] and Quibén and Thome [11]. These maps were developed from experimental observations of the flow regimes of five different refrigerants during evaporation. Nevertheless, despite the progress made in diabatic flow maps, it is acknowledged that there is significant scope for improvement. The availability of more experimental data, and the means to readily acquire this data, can lead to more robust flow maps and, ultimately, more accurate predictive techniques.

Various flow regime identification methods have been used in experimental studies in the literature. One of the most popular, and straightforward, means of identifying a flow regime is to incorporate a sight glass into the geometry of interest, which permits visual observation of the flow pattern. This approach has been the basis for many flow regime investigations, despite the obvious drawback of limited measurement resolution. A sight glass can only provide an instantaneous sighting of the flow regime at the particular location where it is installed, and cannot provide a continuous window into the evolution of the two-phase flow through a geometry. More advanced experimental techniques include signal processing of pressure fluctuations [12], void fraction fluctuations [13], spectral distribution of wall pressure fluctuations [14], pressure gradient variations [15], neutron radiography [16], and electrical conductance probes [17]. However, all of these approaches share a common characteristic - they are expensive and require specialist equipment. The procurement and installation of such equipment can be expensive and time consuming. The methodology being proposed in this paper offers a more simplistic and inexpensive means to identifying two-phase flow regimes, and it is anticipated that the technique can be employed to supplement the flow regime data which currently exists in the literature.

In addition to presenting a novel experimental flow regime identification technique, this paper also seeks to address the deficit of steam condensation flow regime studies in the literature. Indeed, in one of the more recent review papers on the topic of two-phase flows, Cheng et al.

[18] expressed their concerns on this matter by explicitly stating that there is a lack of flow-pattern data for condensation studies in general, and that more studies of in-tube condensation are necessary. There are some data available, but most of this data pertains to refrigerants [19, 20, 21, 22]. Steam data is much less common, which is somewhat surprising given the widespread use of steam condensation in thermal power plant condensers.

There are a limited number of studies, such as that of Chen and Cheng [23] and Louahli-Gualous and Mecheri [24], however, both of these investigations are based around mini channel geometries ( $D_h < 3$  mm) - which are not applicable to conventional condensers in power plants. In response, this study seeks to offer some insight into the two-phase flow regimes expected in steam condensers, by experimentally investigating condensing flows of steam in a horizontal tube at typical Rankine cycle conditions.

## 2. Experimentation

### 2.1. Measurement Architecture

A 25 mm internal diameter aluminium tube, with annular fins on the exterior, formed the basis of this investigation. The tube was finned due to the fact that it was air-cooled, and formed part of a larger investigation into condensation in air-cooled condensers (ACCs) by O'Donovan and Grimes [25]. However, as shown in Figure 1, prior to the extended finned surface being applied, five collinear and equidistant measurement sites were machined along the length of

the outer tube wall. The tube wall was approximately 3.3 mm in thickness, with each site being machined to a depth of approximately 2 mm. Five negative temperature coefficient thermistors, with an accuracy of  $\pm 0.1$  K, were embedded into these sites using high-conductivity thermal paste. The objective was to mount the thermistors as close as was practically possible to the inside tube wall, in an effort to obtain a measurement at that point. As each thermistor was installed in a channel 2 mm deep, a small radial depth of approximately 1.3 mm remained between the thermistor and the inner tube wall. This depth was purposely chosen to minimise thermal resistance, whilst ensuring structural integrity. For the case being presented here, the combined thermal resistance of the  $\sim 1.3$  mm tube wall and  $\sim 0.5$  mm layer of thermal paste was calculated to be  $45 \times 10^{-6}$  K/W. Accordingly, the temperature drop across the wall and thermal paste was almost negligible, relative to the magnitude of temperature drop across the condensate layer. Therefore, these infinitesimal temperature drops were ignored, and it was assumed that each wall thermistor provided a local measurement of the inside wall surface temperature.

A corresponding set of five identical thermistors were mounted along the axial centreline inside the tube, to measure the local steam temperature. These sites inside the tube coincided with those machined into the tube wall, thus providing a platform with which to measure the temperature difference from the core of the tube to the inside tube wall. The thermistors inside the tube were mounted using custom-built

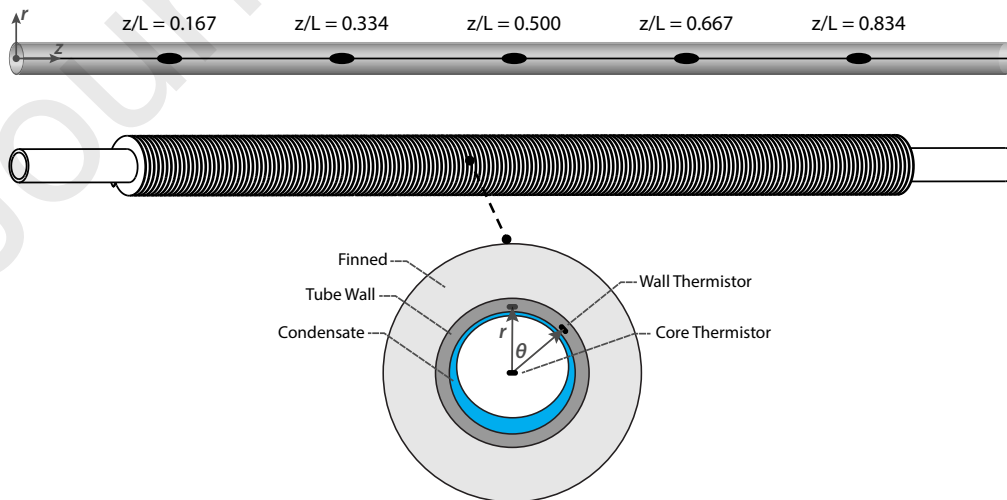


Figure 1: Thermistor arrangement to provide local temperature measurement platform

polycarbonate inserts, which were designed to be minimally-invasive to the flow. Each thermistor - including those embedded in the tube wall - was integrated as a comparator, in parallel with a reference voltage divider, to form a Wheatstone bridge. This circuitry allows for ratiometric measurement, which improves upon the natural sensitivity of thermistors, in addition to providing noise reduction and mitigating against Joule heating. The output voltages from each Wheatstone bridge were acquired, conditioned, and recorded using LabVIEW 2015. The measurement resolution of the arrangement described hitherto was enhanced significantly by the ability to rotate the tube about its central  $z$ -axis. Rotating the tube shifted the measurement platform, as the collinear set of wall thermistors rotated about the fixed core thermistors, through the azimuthal,  $\theta$ , as depicted in the cross-sectional view in Figure 1. This permitted measurement of the temperature difference around the tube circumference, at each axial site along the length of the tube, thereby increasing the measurement resolution to encompass a significant portion of the inner surface area. Although the experimental set-up in this investigation permitted tube rotation, this may not always be possible, particularly in the case of non-circular tubes. In such cases, it is suggested that additional thermistors be mounted in the tube wall to increase measurement resolution to the desired level. The obvious drawback of this approach is the added expense of increased instrumentation. Nevertheless, the authors are currently investigating flow regimes in a tube of rectangular cross-section using this methodology.

The premise of the methodology outlined in this paper is that local temperature difference data (from the tube core to the tube wall) can be used to infer the type of two-phase flow regime. This method of data interpretation is predicated on the fact that the presence of a film of liquid at any point inside the tube is accompanied by a temperature drop from the core to the wall, through that liquid film. A thicker film will result in a larger temperature drop than that arising from a thinner film. Temperature drop through a liquid film has been recognised by many authors as an intrinsic feature of filmwise condensation, and by measuring the local temperature drop around the inner tube circumference, it is possible to infer the distribution of liquid film inside the tube. In fact, this approach is based on the method originally pioneered by Rosson and Meyers [26], who measured point values of condensing film coef-

ficients in a horizontal pipe using local temperature drop data. However, their analysis was limited to a single axial plane. By adopting and expanding upon this method, the local temperature difference measurements presented in this paper should permit prevailing, physically dissimilar flow regimes, such as annular flow and stratified flow, to be distinguished from one another.

## 2.2. Experimental Test Facility

To simulate realistic Rankine cycle air-cooling conditions, the instrumented tube was subjected to a cross-flow of air provided by a bank of eleven axial fans incorporated into a housing with the tube. As the fans contained electronically commutated motors, it was possible to alter and control the air flow rate passing over the tube by adjusting the fan speed. The fans were installed in parallel, which ensured uniform fan speed across the fan bank. Ultimately, this resulted in a uniform air flow rate across the tube. The aerodynamic profile of the fan bank was characterised in a separate experimental program as reported in O'Donovan [27], with Table 1 summarising the range of air flow conditions pertaining to this study.

Parameter	Quantity
$T_\infty$ ( $^\circ\text{C}$ )	19 - 22
$u_a$ ( $\text{m}\cdot\text{s}^{-1}$ )	2.5 - 6.5
$\dot{m}_a$ ( $\text{kg}\cdot\text{s}^{-1}$ )	0.06 - 0.15

Table 1: Cooling conditions employed in this study

As shown in Figure 2, the tube was integrated into a custom-built steam and condensate loop. For all measurements presented in this paper, the tube was fixed in the horizontal position shown. Specialist inlet and exit connections on the tube permitted rotation about its central  $z$ -axis. Steam was generated in a boiler, before passing through a steam separator to remove moisture from the steam and improve the quality. A series of ball valves controlled the steam flow rate entering the tube. The combined effect of the steam separator and throttling across the partially-open valves ensured slightly superheated steam ( $1 - 6 \text{ K} > T_{sat}$ ) at the condenser inlet. Pairs of pressure transducers (with an accuracy of  $\pm 0.08\%$ ) and K-type thermocouples (with an accuracy of  $\pm 0.1 \text{ K}$ ) monitored the steam-side pressure and temperature at various points along the steam and condensate loop. Condensate exiting the tube was subcooled ( $5 - 15 \text{ K} < T_{sat}$ ) for all flow

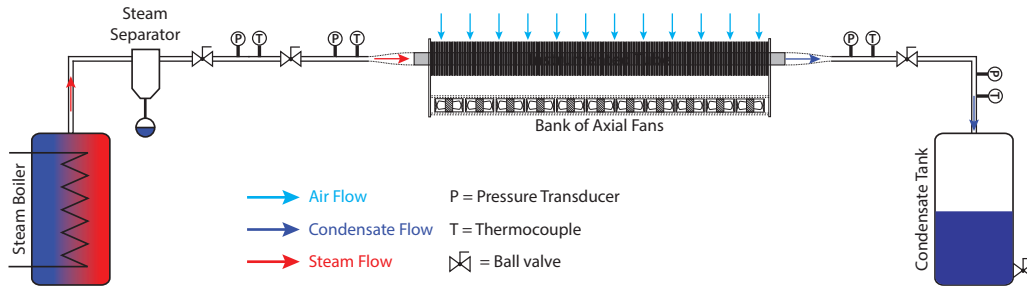


Figure 2: Schematic overview of experimental test facility for two-phase flow experiments

rates investigated herein. Complete condensation was maintained throughout, resulting in a quality variation of  $x = 1$  at the inlet to  $x = 0$  at the exit. Condensate was collected in a condensate tank, and the flow rate was inferred by measuring the mass collected over the recorded collection time period. As steam/condensate flow rate was varied during testing, the air flow rate was adjusted accordingly - in an effort to maintain a constant steam temperature value. This condition was imposed in order to examine the singular effect of steam flow rate on the flow regimes. Table 2 summarises the range of steam/condensate-side conditions for this study.

Parameter	Quantity
$T_{sat}$ ( $^{\circ}\text{C}$ )	39 - 42
$\dot{m}_c$ ( $\text{g}\cdot\text{s}^{-1}$ )	0.42 - 0.94
$P_{sat}$ ( $\text{N}\cdot\text{m}^{-2}$ )	6900 - 8100

Table 2: Steam/condensate-side flow conditions investigated in this study

To ensure that the condensate-side conditions were representative of typical ACC operating conditions, all condensing flows were examined at sub-atmospheric pressure. To satisfy this requirement, the entire experimental facility was designed using specialist vacuum-grade equipment and fittings. Doing so prevented air leakage into the system - which would otherwise tend to occur. Air leakage, or lack thereof, was monitored periodically throughout testing and, as no significant quantities of air were found to be leaking into the system, single-component condensation was sustained throughout.

### 2.3. Experimental Methodology

1. At start-up, the tube was fixed in the horizontal position shown in Figure 2.

2. The rotational angle of the tube was set, ensuring that the wall thermistors were fixed in the desired azimuthal position,  $\theta$ .
3. The connections on the tube inlet and outlet were tightened, fixing the tube in place. The boiler was engaged to produce steam, and all the valves shown in Figure 2 were set to the fully-open position.
4. Steam was released from the boiler and allowed to flow through the steam line and into the condenser - without the fans on. The steam exited the condenser and flowed into the condensate tank, where it was eventually vented to atmosphere. This “purging” procedure served to remove any residual air pockets and/or condensate from the system.
5. Once purging was complete, the valve directly upstream of the condenser inlet and the valve on the condensate tank were closed, leaving a fixed quantity of steam in the condenser. The bank of fans were then set to maximum fan speed, condensing the steam. Eventually the saturation temperature reaches the ambient air temperature and, accordingly, the saturation pressure reduces to its equilibrium value.
6. Steam flow was resumed by opening the inlet valve directly upstream of the condenser. The valve was set to a specific position to fix the steam/condensate mass flow rate. Air flow rate was adjusted until the desired steam temperature was reached.
7. The core and wall temperatures were recorded on LabVIEW. Simultaneously, the temperature and pressure at the condenser inlet and outlet were recorded.
8. The condensate was collected over a specific time period and, when testing at a particular steam flow rate was complete, the tank was separated from the system and placed on a scales where the mass of

- condensate was measured. The mass flow rate was, thus, inferred.
9. Steps 4 - 8 were repeated for a range of steam flow rates - through adjusting the valves in Step 6.
  10. Steps 2 - 9 were repeated for the range of azimuthal positions, through altering the tube rotational angle (Step 2) and adjusting the tube connections (Step 3).

#### 2.4. Data Analysis

The approach and methodology outlined thus far permits measurement of the temperature difference around the tube circumference at each axial site along the length of the tube. This results in a series of measurement points, each one comprised of a core temperature measurement and a corresponding wall temperature measurement. The complete set of measurement points can be compiled to ultimately form a measurement grid, which is a projection of the tube surface area bounded by the measurement points, as shown in Figure 3.

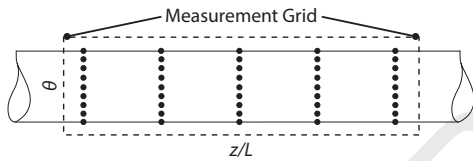


Figure 3: Measurement grid representing the tube surface area enclosed by thermistor sites

The resolution of the grid in this instance is limited by the number of thermistor axial sites - five, and the chosen number of tube rotations - nine. However, the resolution can be increased to the desired level by simply mounting more pairs of core thermistors and wall thermistors along the tube length, and/or employing more tube rotations. Indeed, this is a benefit of the methodology proposed in this paper, whereby the sensor architecture can be customised and tailored to suit the specific requirements and/or application. This can be done at the outset of an experimental program, or retrospectively. The grid that is ultimately generated is presented here with the azimuthal ( $\theta$ ) as the vertical axis, and the axial position ( $z$ ), non-dimensionalised by the tube length ( $L$ ), as the horizontal axis. As will be shown in the results section, this grid can be used to generate contour plots of the temperature difference, from which the flow regime can be inferred.

#### 2.5. Data Uncertainty

The influence of measurement uncertainties on the data presented in this paper has been ac-

counted for using an uncertainty analysis presented by Holman [28], which is an extension of the popular method of Kline and McClintock [29]. This method is based on the specification of the uncertainties in the primary measured data, and the subsequent calculation of uncertainty in the final, desired quantity. Uncertainty in the measurement of temperature, pressure, condensate mass flow rate, and air mass flow rate was  $\pm 0.1$  K,  $\pm 28$  Pa, 5.2%, and 8.1% respectively. Accordingly, the uncertainty in the derived parameters of heat transfer rate, air velocity, and steam quality was estimated as 5.1%, 10.6%, and 8.2%, respectively. In the interest of clarity, the resulting uncertainty bands have been omitted when presenting data.

### 3. Results and Discussion

#### 3.1. Preliminary Results

Prior to any systematic investigation into flow regimes, it was necessary to examine the validity and merit of the proposed experimental approach and associated methodology. Therefore, a suite of preliminary tests were undertaken. These tests were limited to a single, median steam flow rate of  $0.65 \text{ g}\cdot\text{s}^{-1}$ , with the tube undergoing a full rotation about the  $z$ -axis. At each rotational angle, the steam core temperatures and corresponding wall temperatures were simultaneously measured, establishing the temperature difference between the core and the tube wall. Figure 4 presents one such set of measurements, with the temperature difference expressed as a function of the azimuthal angle for a complete rotation.

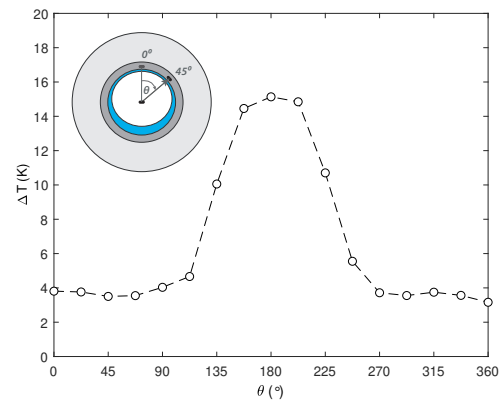


Figure 4: Variation in the measured temperature difference from the steam core to the tube wall around the tube circumference at an axial plane of  $z/L = 0.5$

The premise underlying this study is illustrated in Figure 4, where the shape and magnitude of

the temperature difference profile around the inside of the tube can be interpreted as an indication of the type of two-phase flow regime. Analysing the data from left-to-right, it can be seen that there is a relatively small temperature difference around the top of the tube, i.e.  $0^\circ \leq \theta \leq 90^\circ$ . This temperature difference is the basis for condensation to occur, and remains relatively constant until an angle of  $\theta \approx 115^\circ$  is approached. Hereafter, the temperature difference increases quite dramatically - suggesting that the thickness of the condensate layer on the inside wall is also increasing. The increase in temperature difference subsides and peaks at  $\theta = 180^\circ$ . Once this threshold point is reached, the temperature difference begins to decrease as rotation angle is further increased beyond  $\theta = 180^\circ$ , with the data displaying a symmetrical profile.

Observations from the data presented in Figure 4 imply that the majority of the condensate resides around the bottom of the tube, i.e.  $160^\circ \leq \theta \leq 200^\circ$ , where the largest temperature differences were measured. Indeed, the dramatic increase in temperature difference from the top to the bottom of the tube is consistent with the measurements of Rosson and Meyers [26], who observed an almost linear increase in temperature difference with rotation angle, once  $\theta = 100^\circ$  was reached. In the present study, the measurements suggest that the flow is assuming some quasi-annular flow. This is characterised by a thin film of liquid in the upper portion of the tube, with a thicker condensate pool residing in the bottom of the tube, such

as that depicted in the cross-sectional view of the tube embedded in Figure 4. In an adiabatic flow scenario, this would most likely be classified as a stratified or, perhaps, a stratified-wavy flow. However, as the vapour is continually condensing in this case, a thin film of liquid is invariably formed which coats the entire perimeter of the inside tube wall. Therefore, this leads to a flow topology which resembles annular flow, albeit with a thicker film in the bottom portion of the tube - a scenario which some authors have described as quasi-annular.

The measurements presented in Figure 4 pertain to a single axial location ( $z/L = 0.5$ ). The full set of measurements for each designated axial site along the length of the tube, at the same steam flow rate of  $0.65 \text{ g}\cdot\text{s}^{-1}$ , are presented in Figure 5. For a particular tube rotation, the temperature difference from the steam core to the tube wall was acquired simultaneously at each axial plane. The data is presented in the form of a polar plot - where the qualitative distribution, rather than the actual quantitative distribution, is of interest in this instance. Accompanying the polar plots in Figure 5 is a schematic of the finned tube - to provide an overview of the measurement sites.

The data presented in Figure 5 illustrates a number of prominent characteristics, from which the flow topology can be inferred. Perhaps the most obvious characteristic is the multidimensional nature of the temperature difference measurements. An increase in temperature difference is generally seen to occur in two-dimensions; along the axial direction, and around the tube

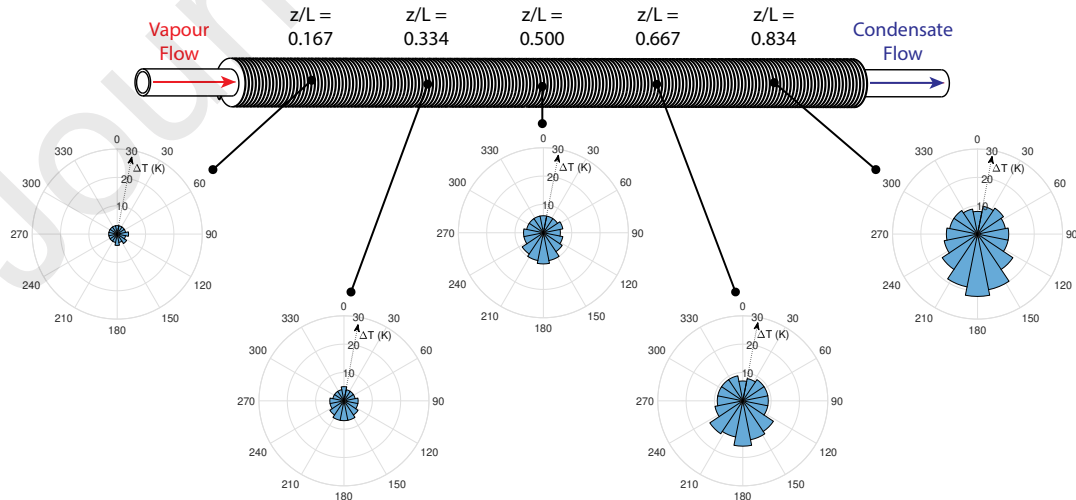


Figure 5: Variation in measured temperature difference from the steam core to the tube wall around the tube circumference at all axial planes investigated at a median steam flow rate of  $0.65 \text{ g}\cdot\text{s}^{-1}$

circumference from the top of the tube to the bottom. The increase in temperature difference along the axial length is an intrinsic feature of complete condensation. Inherently, as steam condenses along the length of the tube, the heat transfer rate decreases. This reduction in heat transfer is manifested by an increase in the temperature difference from the steam core to the inner tube wall. Therefore, for a given azimuthal position, the temperature difference generally increases in the downstream direction from tube inlet to outlet. The polar plots in Figure 5 are purposefully arranged so that each successive plot depicts the overall trend of temperature difference increasing for all points along the length of the tube.

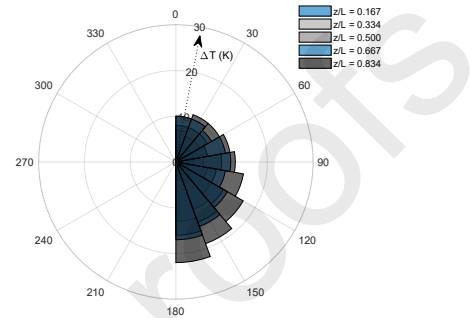
It is also a feature of the data in Figure 5 that the largest temperature differences are consistently located in the vicinity of the bottom of the tube. This is almost always the case, apart from the data presented in the polar plot at  $z/L = 0.167$ , at which point it is unlikely that an appreciably large condensate pool exists to cause an excessive temperature drop at the bottom of the tube. However, the fact that the largest temperature differences exist around the bottom of the tube in all other cases offers compelling evidence that a substantial liquid pool resides there, since it is well recognised that temperature drop through a condensate film is analogous to film thickness. The temperature difference at the bottom also increases along the axial direction, suggesting that the liquid pool is growing in thickness along the tube length. Intuitively this characteristic might be expected but, nonetheless, confirms that as condensation progresses along the length of the tube, the resulting condensate tends to accumulate and grow along the bottom portion of the tube as more mass is transferred. Again, this implies that a quasi-annular or stratified flow regime is the dominant two-phase morphology for the conditions investigated in this study.

A major outcome of the preliminary testing was the observation of symmetry in the data. As can be clearly seen in Figures 4 and 5, the data is symmetrical about the  $r$ -axis centreline. This symmetry was also apparent at all other flow rates investigated, and was confirmed by intermittent checks. However, such measurements are excluded here for the purposes of clarity as the axisymmetry is sufficiently illustrated by Figure 4 and 5. Nevertheless, due to the axisymmetry, subsequent measurements were abridged as only a half-tube rotation ( $0^\circ \leq \theta \leq 180^\circ$ ) was required.

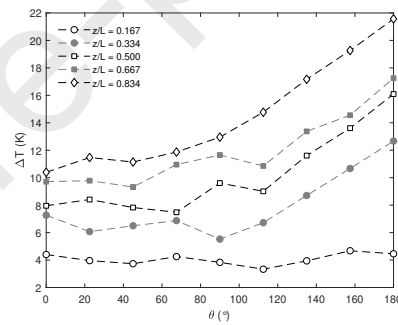
### 3.2. Flow Regime Identification

#### 3.2.1. Time-Averaged Measurements

To supplement the qualitative distributions given in Figure 5, the remaining data is presented in a more quantitative format in Figures 6 - 10. This data consists of temperature difference measurements around the tube circumference at each axial plane, for the full range of steam mass flow rates considered in this study.

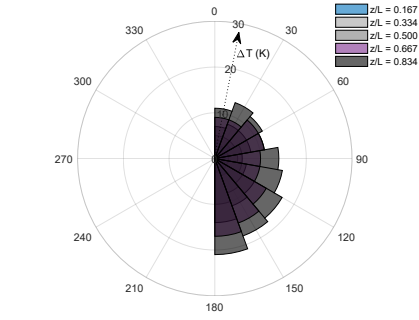


(a) Qualitative distribution

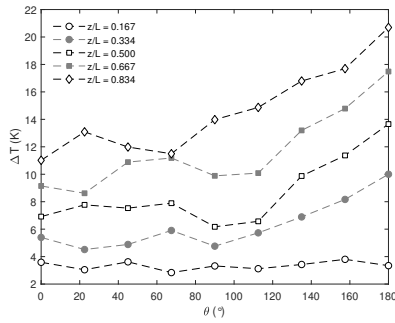


(b) Quantitative distribution

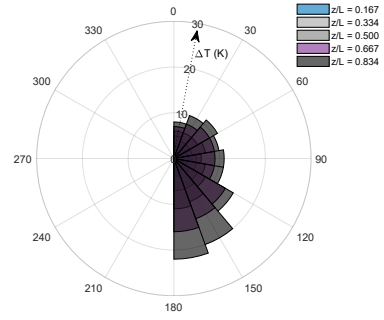
Figure 6: Temperature difference measurements acquired at  $\dot{m}_c = 0.42 \text{ g}\cdot\text{s}^{-1}$ . Conditions were:  $T_{sat} = 40^\circ\text{C}$ ,  $P_{sat} = 7350 \text{ Pa}$ ,  $\dot{Q} = 980 \text{ W}$ ,  $\dot{m}_a = 0.062 \text{ kg}\cdot\text{s}^{-1}$



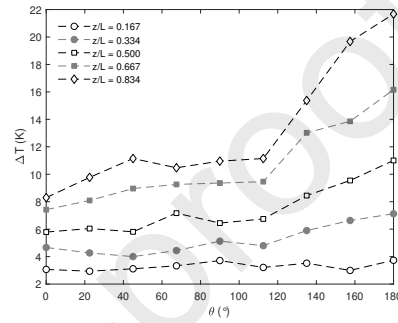
(a) Qualitative distribution



(b) Quantitative distribution



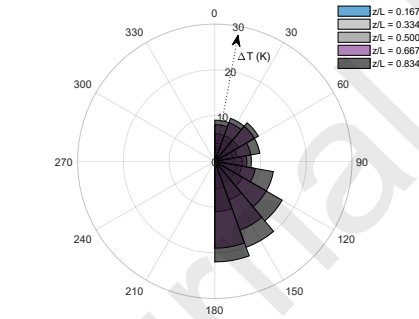
(a) Qualitative distribution



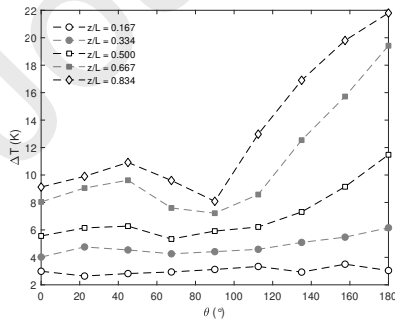
(b) Quantitative distribution

Figure 7: Temperature difference measurements acquired at  $\dot{m}_c = 0.57 \text{ g}\cdot\text{s}^{-1}$ . Conditions were:  $T_{sat} = 39 \text{ }^\circ\text{C}$ ,  $P_{sat} = 6900 \text{ Pa}$ ,  $\dot{Q} = 1300 \text{ W}$ ,  $\dot{m}_a = 0.084 \text{ kg}\cdot\text{s}^{-1}$

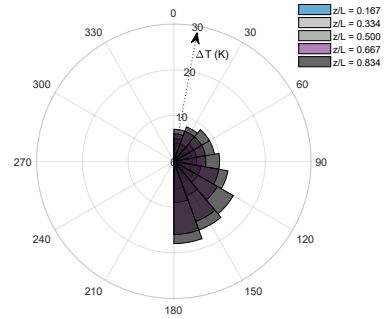
Figure 8: Temperature difference measurements acquired at  $\dot{m}_c = 0.65 \text{ g}\cdot\text{s}^{-1}$ . Conditions were:  $T_{sat} = 40 \text{ }^\circ\text{C}$ ,  $P_{sat} = 7350 \text{ Pa}$ ,  $\dot{Q} = 1500 \text{ W}$ ,  $\dot{m}_a = 0.093 \text{ kg}\cdot\text{s}^{-1}$



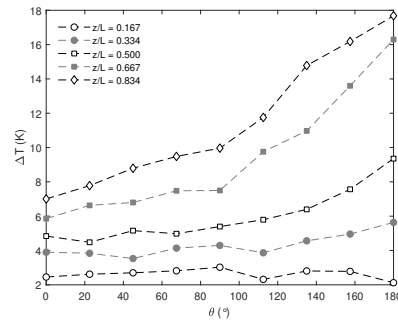
(a) Qualitative distribution



(b) Quantitative distribution



(a) Qualitative distribution



(b) Quantitative distribution

Figure 9: Temperature difference measurements acquired at  $\dot{m}_c = 0.81 \text{ g}\cdot\text{s}^{-1}$ . Conditions were:  $T_{sat} = 41 \text{ }^\circ\text{C}$ ,  $P_{sat} = 7750 \text{ Pa}$ ,  $\dot{Q} = 1850 \text{ W}$ ,  $\dot{m}_a = 0.12 \text{ kg}\cdot\text{s}^{-1}$

Figure 10: Temperature difference measurements acquired at  $\dot{m}_c = 0.94 \text{ g}\cdot\text{s}^{-1}$ . Conditions were:  $T_{sat} = 42 \text{ }^\circ\text{C}$ ,  $P_{sat} = 8100 \text{ Pa}$ ,  $\dot{Q} = 2150 \text{ W}$ ,  $\dot{m}_a = 0.15 \text{ kg}\cdot\text{s}^{-1}$

It is clear that the measurements presented in Figures 6 - 10 depict the same overall trends as those described thus far. Apart from some notable exceptions, the temperature difference tends to increase as rotation angle is increased in all cases. Ultimately, this characteristic can be interpreted as an increase in the condensate film thickness from the top to the bottom of the tube. The primary exception to this trend is the data obtained at the axial plane of  $z/L = 0.167$ . Across all steam flow rates examined, the temperature difference profile at  $z/L = 0.167$  remains relatively static, and does not tend to increase in the same manner as the data obtained at other axial locations. This static profile is attributed to a combination of large vapour velocities and a thin film of liquid near the tube inlet. As  $z/L = 0.167$  is so close to the tube inlet, condensation will not have sufficiently progressed to produce an appreciable quantity of liquid - resulting in a thin film instead of a thicker pool. Coupled to this are the large vapour velocities at the tube inlet, which will tend to distribute this thin film evenly around the tube wall. With a relatively uniform film of liquid, the temperature drop through it will be constant, or static as seen in the data presented in Figures 6 - 10.

In addition to the exception of the  $z/L = 0.167$  data, there are also some irregularities in the other data sets which are characterised by a deviation from the general trend of temperature difference increasing with rotation angle. This is particular apparent in Figure 9, where it can be seen that there are local minima in the temperature difference measurements for  $z/L = 0.667$  and  $z/L = 0.834$  occurring at  $\theta \approx 90^\circ$ . These local minima are quite a departure from the general trend observed elsewhere. This behaviour may be explained by considering the conditions. Firstly, the axial locations of  $z/L = 0.667$  and  $z/L = 0.834$  are sufficiently downstream so that condensation will have progressed to the point where an appreciable pool of liquid will have developed. Additionally, due to the higher steam flow rate of  $0.81 \text{ g}\cdot\text{s}^{-1}$ , it is likely that the vapour velocity will be large enough to disturb and deform the liquid-vapour interface, resulting in intermittent wavy motion. Indeed, this has been reported by Carey [30] as a feature of stratified flow when the flow rate is increased, whereby the interface becomes ‘‘Helmholtz unstable’’ due to strong vapour shear acting on a pool of liquid. The troughs associated with the wavy motion could be responsible for the local minima values seen in the temperature profiles of Figure 9.

Figures 6 - 10 also demonstrate the effect of steam flow rate on the magnitude of temperature difference. In general, an increase in steam flow rate appears to reduce the magnitude of temperature difference, for any given azimuthal position. This is illustrated most clearly at  $\theta > 120^\circ$ , where it is suspected that liquid accumulating on the tube wall is disturbed and ‘‘thinned’’ by the increased vapour velocity accompanying the increased steam flow rate. This behaviour ultimately augments heat transfer and reduces the temperature difference. At  $\theta < 120^\circ$ , the condensate film will not be as substantial and, thus, the effect of steam flow rate on temperature difference is not seen to the same extent.

Based on the results presented thus far in Figures 6 - 10, it could be deduced that the two-phase flow morphology consists of a thin film of liquid coating the majority of the inside perimeter of the tube, with a thicker pool residing in the bottom. This can be thought of as quasi-annular, or annular-stratified flow - as coined by Carey [30]. Similar findings were also reported by Guo et al. [31], who investigated the steam-liquid distribution during condensation via electrical capacitance tomography, at flow rates similar to those examined in this study.

### 3.2.2. Instantaneous Measurements

An issue, admittedly, with the proposed experimental technique for identifying the flow regime is that it only provides a means with which to infer the regime, with the flow regime never being explicitly confirmed. Nevertheless, sufficient analysis of acquired data can lead to valuable insight on the nature of the flow. As with most data acquired over a period of time, the data presented hitherto is time-averaged. However, Figure 11 presents a sample of instantaneous data, acquired over a thirty second time interval during experimentation. Examination of this data provides further insight into the flow regime.

The most noticeable feature of Figure 11 is the progression of scatter in the data from the measurements taken around the top of the tube to those taken near the bottom. It can be seen in Figures 11a - 11c, which represent the upper portion of the tube, that the data is relatively smooth across the time period for both steam flow rates presented. This implies that the condensing film is relatively consistent at these measurement points. However, as shown in Figure 11d, measurements near the bottom of the tube exhibited significantly more scatter. These large fluctuations are attributed to

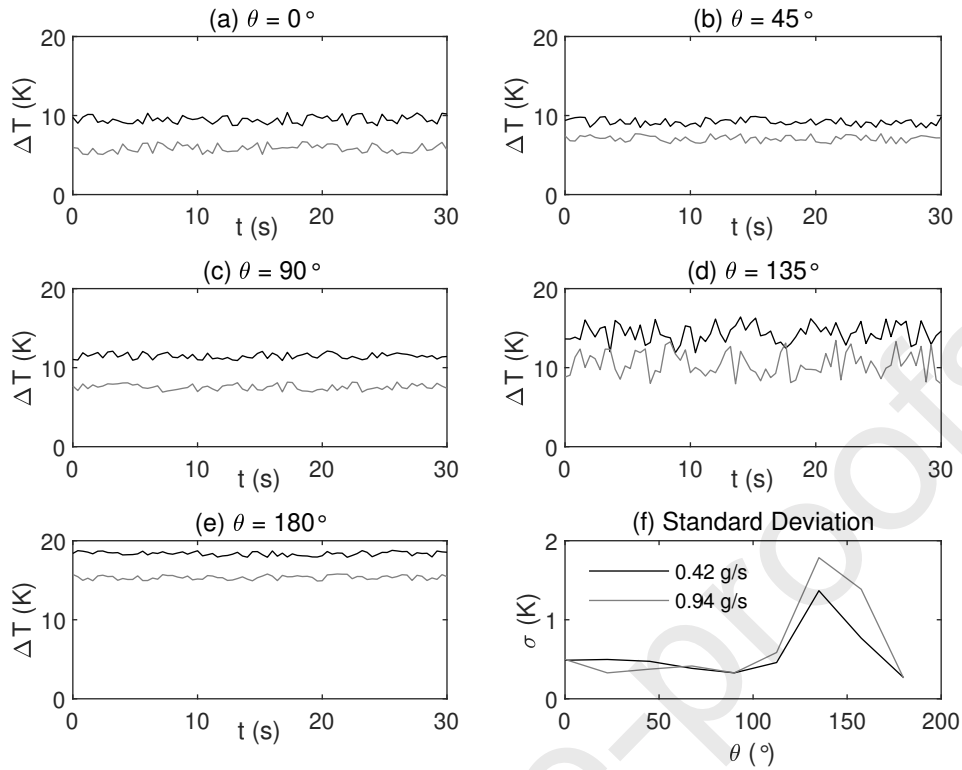


Figure 11: Sample of instantaneous measurements

the onset of waves in the liquid phase and, inherently, the effect of waves will only be appreciable towards the bottom of the tube where the liquid film resides. A similar phenomenon was also observed by Rosson and Meyers [26], who found the effect of waves to be most pronounced at approximately  $\theta = 120^\circ$ . Rosson and Meyers presented some of their own temperature measurements, and stated that the irrational variation in the temperature difference histories must be due to the action of waves moving up and around the inside tube perimeter in an intermittent fashion. The presence of a thicker film of liquid at a measurement point, albeit for a short period of time, will give rise to a larger, momentarily temperature drop at that point. This is manifested in the measurements presented in Figure 11d.

Figure 11e presents the data from the extremity of  $\theta = 180^\circ$ , which appears qualitatively similar to that presented in Figures 11a - 11c. At  $\theta = 180^\circ$ , the measurement point is most likely coated by a consistent pool of liquid - unaffected by surface waves. Hence, the data acquired during the thirty second time interval exhibits few fluctuations and little scatter. Ultimately, the scatter in the acquired data is

quantified by the standard deviation from the mean given in Figure 11f. This plot contains data points determined from temperature difference histories at tube rotation angles which, to preserve clarity, were not included in Figure 11. Nevertheless, this data compliments that already presented and, for both steam flow rates, it is clear that the greatest deviations occur before the bottom of the tube is reached. In fact, there is a noticeable maximum in the standard deviation at  $\theta = 135^\circ$ , which suggests that waves are particularly prominent at this angular position in the tube. It is also interesting to note that the standard deviation is generally larger for the higher steam flow rate - possibly due to the higher vapour velocities and the subsequent disturbances of the condensate. Even though only two steam flow rates were presented here, they were deemed to be representative of the entire range as  $0.42 \text{ g}\cdot\text{s}^{-1}$  and  $0.94 \text{ g}\cdot\text{s}^{-1}$  were the smallest and largest steam flow rates investigated, respectively. Therefore, the wavy nature of the flow deduced from the data at those steam flow rates is expected to be a feature across all intermediary flow rates. Ultimately, the instantaneous data presented in Figure 11 appears to indicate a wavy ele-

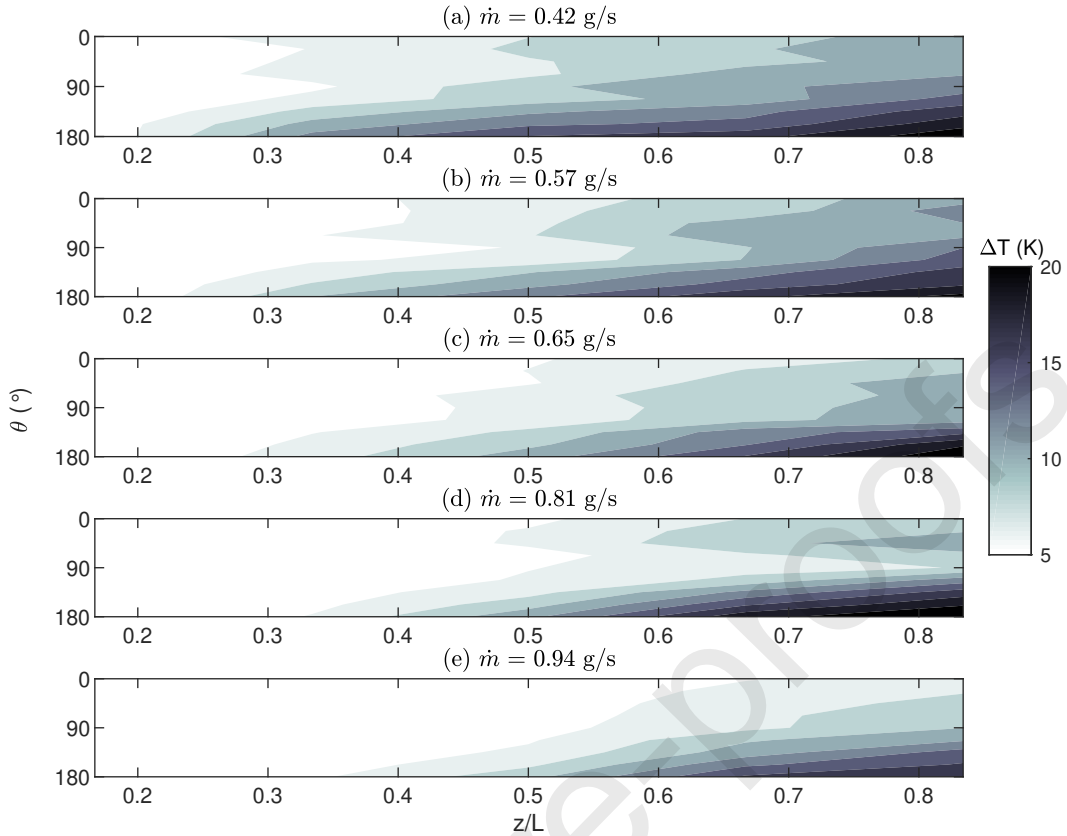


Figure 12: Contour flow maps deduced from local temperature difference measurements

ment to the stratified-annular flow topology inferred from the previous time-averaged measurements.

### 3.3. Contour Flow Maps

The qualitative, and quantitative, temperature difference distribution around the tube circumference and along the tube length is best depicted by employing the measurement grid shown previously in Figure 3. Using this grid, the local temperature difference measurements can be plotted and projected from the tube surface area bounded by the measurement points, with the space between points being interpolated to give a fully-realised contour plot. Ultimately, it is proposed that this contour plot can be interpreted as a time-averaged flow map. Figure 12 presents the contour maps for all steam flow rates investigated in this study.

Interpretation of the flow maps, to identify the prevailing flow regime, is predicated on the measured temperature difference being proportional to the thickness of the liquid film. As can be seen in Figure 12, the temperature differences are smallest near the inlet to the tube ( $z/L = 0.167$ ), and increases progressively in the axial direction. In addition to the increase in the

axial direction, the temperature difference also increases in the azimuthal direction, from the top to the bottom of the tube, as exhibited by previous data. This azimuthal increase in temperature difference was not apparent near the tube inlet and was only measurable, as an appreciable temperature difference, at downstream locations. Thus, it was suggested that the condensate which was forming was accumulating around the bottom perimeter of the tube in downstream regions, thereby contributing a greater temperature drop through that thicker condensate. As indicated by the contour levels in Figure 12, the increases in temperature difference in the axial direction is more pronounced near the bottom of the tube compared to the top.

Based on the qualitative temperature difference distributions shown in Figure 12, and interpreting these measurements to identify the two-phase condensing flow morphology through the tube, an annular flow regime could be proposed to be present near the inlet to the tube, with the flow assuming a quasi-annular (annular with a stratified layer) in the downstream regions. The inference of annular flow can be justified by the approximate uniform distribution of temperat-

ure difference around the circumference in the upstream regions. In the downstream regions, however, the distribution of temperature difference around the circumference is skewed, with an unfavourable gradient towards the bottom of the tube implying a deviation from the symmetrical annular flow regime to a more asymmetrical stratified layer of liquid.

#### 4. Conclusions

A novel experimental measurement technique for identifying the predominant two-phase flow regime for a diabatic flow in a horizontal, circular tube was presented in this paper. The diabatic flow of interest was condensing flows of steam, nevertheless, it is proposed that the methodology outlined can be applied to other scenarios. The approach was based on the ability to acquire local temperature difference measurements, around the tube perimeter, from bespoke instrumentation. The temperature difference measurements were analogous to the condensate film thickness, thus providing a means of inferring the flow regime. The local measurements from around the tube circumference, and along the tube length, were projected onto a measurement grid and, ultimately, were presented in the form of contour plots to visualise the flow through the tube. Results show that, for all steam flow rates investigated in this study, an annular flow exists nearest the tube inlet, with this deviating to a annular-stratified regime towards the tube exit. It is difficult to quantitatively, or qualitatively, compare the results in this study with other findings - mainly due to a lack of similar studies. The vast majority of studies on two-phase flows in round tubes are for a vertical tube configuration, which are considerably easier to characterise due to nature of the set-up which naturally promotes an annular flow regime. Horizontal tube configurations are complicated by the influence of gravity and the tendency for stratification of the flow. Furthermore, almost all studies on horizontal, or slightly inclined, tubes employ some type of refrigerant as the working fluid. Hence, the void in current literature is partly alleviated by the measurements presented in this study. Although there is still some ambiguity in classifying this regime, the experimental methodology certainly allows for drastically dissimilar flow regimes to be differentiated and, ultimately, dis-counted.

#### References

#### References

- [1] R. Lockhart, R. Martinelli, Proposed correlation of data for isothermal two-phase, two-component flow in pipes, *Chem. Eng. Prog* 45 (1949) 39–48.
- [2] D. Chisholm, A theoretical basis for the lockhart-martinelli correlation for two-phase flow, *International Journal of Heat and Mass Transfer* 10 (1967) 1767–1778.
- [3] L. Friedel, Improved friction pressure drop correlation for horizontal and vertical two-phase pipe flow, *Proc. of European Two-Phase Flow Group Meet.*, Ispra, Italy, 1979 (1979).
- [4] H. Müller-Steinhagen, K. Heck, A simple friction pressure drop correlation for two-phase flow in pipes, *Chemical Engineering and Processing: Process Intensification* 20 (1986) 297–308.
- [5] J. M. Quibén, J. R. Thome, Flow pattern based two-phase frictional pressure drop model for horizontal tubes, part ii: New phenomenological model, *International Journal of Heat and Fluid Flow* 28 (2007) 1060–1072.
- [6] O. Baker, Design of pipelines for the simultaneous flow of oil and gas, in: *Fall Meeting of the Petroleum Branch of AIME, Society of Petroleum Engineers*, 1954.
- [7] G. F. Hewitt, D. Roberts, Studies of two-phase flow patterns by simultaneous X-ray and flash photography, *Technical Report, Atomic Energy Research Establishment Harwell (United Kingdom)*, 1969.
- [8] J. Mandhane, G. Gregory, K. Aziz, A flow pattern map for gas-liquid flow in horizontal pipes, *International Journal of Multiphase Flow* 1 (1974) 537–553.
- [9] Y. Taitel, A. Dukler, A model for predicting flow regime transitions in horizontal and near horizontal gas-liquid flow, *AIChE Journal* 22 (1976) 47–55.
- [10] N. Kattan, J. Thome, D. Favrat, Flow boiling in horizontal tubes: Part 1—development of a diabatic two-phase flow pattern map, *Journal of Heat Transfer* 120 (1998) 140–147.
- [11] J. M. Quibén, J. R. Thome, Flow pattern based two-phase frictional pressure drop model for horizontal tubes. part i: Diabatic and adiabatic experimental study, *International Journal of Heat and Fluid Flow* 28 (2007) 1049–1059.
- [12] G. Matsui, Identification of flow regimes in vertical gas-liquid two-phase flow using differential pressure fluctuations, *International journal of multiphase flow* 10 (1984) 711–719.
- [13] E. W. Jassim, T. A. Newell, J. C. Chato, Probabilistic determination of two-phase flow regimes in horizontal tubes utilizing an automated image recognition technique, *Experiments in Fluids* 42 (2007) 563–573.
- [14] J. Drahoš, J. Čermák, K. Selucký, L. Ebner, Characterization of hydrodynamic regimes in horizontal two-phase flow part ii: Analysis of wall pressure fluctuations, *Chemical Engineering and Processing: Process Intensification* 22 (1987) 45–52.
- [15] N. K. Tutu, Pressure fluctuations and flow pattern recognition in vertical two phase gas-liquid flows, *International Journal of Multiphase Flow* 8 (1982) 443–447.
- [16] A. Geiger, A. Tsukada, E. Lehmann, P. Vontobel, A. Wokaun, G. Scherer, In situ investigation of two-phase flow patterns in flow fields of pefcs using neutron radiography, *Fuel Cells* 2 (2002) 92–98.

- [17] D. Barnea, O. Shoham, Y. Taitel, Flow pattern characterization in two phase flow by electrical conductance probe, *International Journal of Multiphase Flow* 6 (1980) 387–397.
- [18] L. Cheng, G. Ribatski, J. Thome, Two-phase flow patterns and flow-pattern maps: Fundamentals and applications, *Applied Mechanics Reviews* 61 (2008) 050802.
- [19] J. El Hajal, J. Thome, A. Cavallini, Condensation in horizontal tubes, part 1: two-phase flow pattern map, *International Journal of Heat and Mass Transfer* 46 (2003) 3349–3363.
- [20] L. Liebenberg, J. R. Thome, J. P. Meyer, Flow visualization and flow pattern identification with power spectral density distributions of pressure traces during refrigerant condensation in smooth and microfin tubes, *Journal of Heat Transfer* 127 (2005) 209–220.
- [21] J. A. Olivier, L. Liebenberg, J. R. Thome, J. P. Meyer, Heat transfer, pressure drop, and flow pattern recognition during condensation inside smooth, helical micro-fin, and herringbone tubes, *International Journal of Refrigeration* 30 (2007) 609–623.
- [22] R. Suliman, L. Liebenberg, J. P. Meyer, Improved flow pattern map for accurate prediction of the heat transfer coefficients during condensation of r-134a in smooth horizontal tubes and within the low-mass flux range, *International Journal of Heat and Mass Transfer* 52 (2009) 5701–5711.
- [23] Y. Chen, P. Cheng, Condensation of steam in silicon microchannels, *International Communications in Heat and Mass Transfer* 32 (2005) 175–183.
- [24] H. Louahlia-Gualous, B. Mecheri, Unsteady steam condensation flow patterns inside a miniature tube, *Applied Thermal Engineering* 27 (2007) 1225–1235.
- [25] A. O’Donovan, R. Grimes, Pressure drop analysis of steam condensation in air-cooled circular tube bundles, *Applied Thermal Engineering* 87 (2015) 106–116.
- [26] H. Rosson, J. Meyers, Point values of condensing film coefficients inside a horizontal tube, in: *Chemical Engineering Progress Symposium Series*, volume 61, 1965, pp. 190–199.
- [27] A. O’Donovan, *On The Thermal and Fluidic Characteristics of Steam Condensation in an Air-Cooled Condenser*, Ph.D. thesis, University of Limerick, Limerick, Ireland, 2015.
- [28] J. P. Holman, *Experimental Methods for Engineers*, seventh ed., McGraw-Hill, 2001.
- [29] S. Kline, F. McClintock, Describing uncertainties in single-sample experiments, *Mechanical Engineering* 75 (1953) 3–8.
- [30] V. Carey, *Liquid-Vapor Phase-Change Phenomena*, 2nd ed., Taylor & Francis, New York, 2008.
- [31] C. Guo, T. Wang, X. Hu, D. Tang, Experimental and theoretical investigation on two-phase flow characteristics and pressure drop during flow condensation in heat transport pipeline, *Applied Thermal Engineering* 66 (2014) 365–374.

## Conflict of Interest

No potential conflict of interest was reported by the authors.

Journal Pre-proofs

## Credit Author Statement

- Alan O'Donovan: Conceptualization, Data curation, Formal analysis, Investigation, Methodology, Validation, Visualization, Writing – original draft
- Ronan Grimes: Funding acquisition, Project administration, Resources, Supervision, Writing – review & editing.

Journal Pre-proofs

## Highlights

- Novel two-phase flow regime identification technique is presented
- Analysis of local temperature data allows predominant flow regimes to be inferred
- Flow patterns for condensing flows of steam are presented
- Annular flow nearest tube inlet progresses to stratified flow at tube exit

Journal Pre-proofs